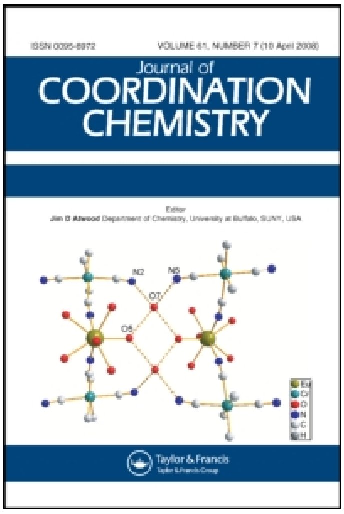

Journal of Coordination Chemistry
Publication details, including instructions for authors and subscription information:
http://www.informaworld.com/smpp/title~content=t713455674

Coordination Compounds of Strontium: Syntheses, Characterizations, and Crystal Structures of $[Sr(\mu\text{-}ONc)_2(HONc)_4]_2$ and $Sr_5(\mu_4\text{-}O)(\mu_3\text{-}ONep)_4(\mu\text{-}ONep)_4(HONep)(solv)_4$ ($ONc = O_2CCH_2CMe_3$; $Nep = CH_2CMe_3$; solv = Tetrahydrofuran or 1-Methyl-Imidazole)

Timothy J. Boyle[a]; Cory J. Tafoya[a]; Brian L. Scott[b]; Joseph W. Ziller[c]
[a] Sandia National Laboratories, Department 1846, Advanced Materials Laboratory, 1001 University Boulevard S.E., Albuquerque, NM, USA [b] Los Alamos National Laboratories, CST-18, Chemical Science and Technology Division - X-ray Diffraction Laboratory, Los Alamos, NM, USA [c] Department of Chemistry, University of California, Irvine, CA, USA

To cite this Article Boyle, Timothy J. , Tafoya, Cory J. , Scott, Brian L. and Ziller, Joseph W.(2000) 'Coordination Compounds of Strontium: Syntheses, Characterizations, and Crystal Structures of $[Sr(\mu\text{-}ONc)_2(HONc)_4]_2$ and $Sr_5(\mu_4\text{-}O)(\mu_3\text{-}ONep)_4(\mu\text{-}ONep)_4(HONep)(solv)_4$ ($ONc = O_2CCH_2CMe_3$; $Nep = CH_2CMe_3$; solv = Tetrahydrofuran or 1-Methyl-Imidazole)', Journal of Coordination Chemistry, 51: 2, 361 — 378

To link to this Article: DOI: 10.1080/00958970008055141

URL: http://dx.doi.org/10.1080/00958970008055141

J. Coord. Chem., 2000, Vol. 51, pp. 361–378
Reprints available directly from the publisher
Photocopying permitted by license only

Published by license under
the Gordon and Breach Science
Publishers imprint.
Printed in Malaysia.

COORDINATION COMPOUNDS OF STRONTIUM: SYNTHESES, CHARACTERIZATIONS, AND CRYSTAL STRUCTURES OF $[Sr(\mu\text{-}ONc)_2(HONc)_4]_2$ AND $Sr_5(\mu_4\text{-}O)(\mu_3\text{-}ONep)_4(\mu\text{-}ONep)_4(HONep)(solv)_4$ $(ONc = O_2CCH_2CMe_3;\ Nep = CH_2CMe_3;$ solv = TETRAHYDROFURAN OR 1-METHYL-IMIDAZOLE)

TIMOTHY J. BOYLE[a,*], CORY J. TAFOYA[a],
BRIAN L. SCOTT[b] and JOSEPH W. ZILLER[c]

[a]*Sandia National Laboratories, Department 1846, Advanced Materials Laboratory, 1001 University Boulevard S.E., Albuquerque, NM 87106, USA;* [b]*Los Alamos National Laboratories, CST-18, Chemical Science and Technology Division – X-ray Diffraction Laboratory, Los Alamos, NM 87545, USA;* [c]*Department of Chemistry, University of California – Irvine, CA 92717, USA*

(Received 10 July 1999; Revised 15 September 1999; In final form 20 January 2000)

We have synthesized and characterized two novel Sr compounds: $[Sr(\mu\text{-}ONc)_2(HONc)_4]_2$ (**1**, $ONc = O_2CCH_2CMe_3$), and $Sr_5(\mu_4\text{-}O)(\mu_3\text{-}ONep)_4(\mu\text{-}ONep)_4(HONep)(solv)_4$ [$ONep = OCH_2CMe_3$, solv = tetrahydrofuran (THF), **2a**; 1-methyl-imidazole (MeIm), **2b**], that demonstrate increased solubility in comparison to the commercially available Sr precursors. The two metal centers of **1** share four unidentate bridging μ-ONc ligands and complete their octahedral geometry through coordination of four monodentate terminal HONc ligands. The structural arrangement of the central core of **2a** and **2b** are identical, wherein four octahedral Sr atoms are arranged in a square geometry around a μ_4-O ligand. An additional seven-coordinated Sr atom sits directly atop the μ_4-O to form a square-pyramidal arrangement of the Sr atoms, but the apical Sr–O distance is too long to be considered a bond. In solution, compound **1** is disrupted forming a monomer but **2a** and **2b** retain their structures.

Keywords: Metal alkoxide; strontium; neo-pentoxide; *t*-butyl acetate

---

[*] Corresponding author. Tel.: 505 272 7625. Fax: 505 272 7304.

INTRODUCTION

Thin films of strontium-containing electroceramic materials are of increased interest for the development of electronic devices. In particular, two Sr-containing materials that have been recently investigationed are $SrBi_2Ta_2O_9$ (SBT) and $(Ba_{1-x},Sr_x)TaO_3$ (BST).[1-25] SBT is being considered for use in non-volatile memory devices due to its low fatigue on platinum electrodes.[11-25] BST is of interest as a tunable high dielectric constant material for a number of telecommunication applications.[2,6-10] While many routes exist to generate thin films, solution routes (*i.e.*, dip or spin-coating) are often favored since they are simple, flexible, inexpensive, and in-line with existing semi-conductor technologies.[1] Solution routes involve three steps: (i) dissolution of a precursor in a solvent, (ii) deposition of precursor solution onto a substrate, and (iii) thermal treatment to convert the metallo-organic species to the ceramic phase. Both $Sr(OAc)_2$ ($OAc = O_2CMe$) and $Sr(OPr^i)_2$ ($OPr^i = OCHMe_2$) are common starting materials for solution methods to SBT and BST since they are commercially available; however, their poor solubility in standard organic solvents greatly limits the development of alternative precursor solutions and frustrates optimization of the properties of the final ceramic material.

We have synthesized novel Sr precursors that demonstrate increased solubility for the production of thin films of SBT and BST.[1-5] Our investigations have focused on small chain (≤ 6 carbons) non-aromatic alkoxide (OR) and carboxylic acetate (ORc) precursors. The small carbon count is necessary to maintain low processing temperatures and to minimize residual carbon content. At the same time, increasing the steric bulk of the pendant hydrocarbon chains increases the solubility and reduces oligomerization.[26] Therefore, by judiciously choosing the appropriate ligands the solubility of the precursor can be increased without affecting the processing temperature.

One pendant hydrocarbon chain that has proven to be extremely beneficial in generating high quality films at low processing temperatures is the neo-pentyl ($CH_2CMe_3 = Nep$) moiety.[1,2,27] The Nep chain is attractive for solution routes to materials for two reasons: (i) the β-hydrogens allow for "cross-linking" of metal centers upon exposure to atmospheric humidity, yielding uniform films and (ii) the *t*-butyl moiety, due to steric hindrance, minimizes oligomerization and increases the solubility of the modified species. Figure 1 is a schematic representation of two of the commercially available ligands that employ the Nep hydrocarbon moiety in their structures: $HO_2CCH_2CMe_3$ (HONc) and $HOCH_2CMe_3$ (HONep).

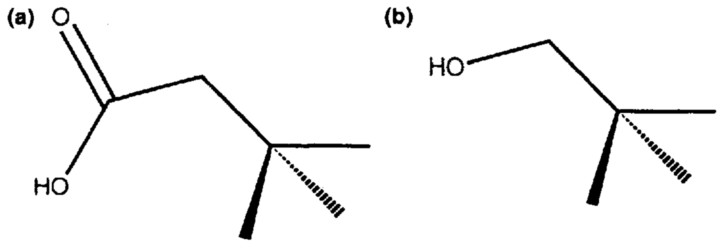

FIGURE 1 Schematic representation of ligands (a) $HO_2C\text{-}CH_2CMe_3$ (HONc) and (b) $HO\text{-}CH_2CMe_3$ (HONep).

This report details the syntheses, characterizations, and solution behaviors of novel Sr precursors ligated by the ONc and ONep moieties. The resultant products were identified by single crystal X-ray diffraction as $[Sr(\mu\text{-}ONc)_2(HONc)_4]_2$ (**1**) and $Sr_5(\mu_4\text{-}O)(\mu_3\text{-}ONep)_4(\mu\text{-}ONep)_4(HONep)(solv)_4$ [solv = THF, **2a**; solv = MeIm and $\cdot(MeIm)_2(C_6H_8)$ **2b**] and found to be soluble in standard organic solvents. These precursors have been successfully integrated into novel precursor solution routes to thin films of SBT and BST, details of which have been presented elsewhere.[2,14,28]

EXPERIMENTAL

All compounds described below were handled with rigorous exclusion of air and water using standard Schlenk, vacuum line, and glovebox techniques. All solvents were freshly distilled and dried from sodium benzophenone ketyl prior to use. Solution NMR spectra were obtained on a Bruker 400 MHz spectrometer and referenced against the residual protons in toluene-d_8. FT-IR data were obtained on a Nicolet Magna System 550 spectrometer. Thermal gravimetric analysis/differential thermal analysis (TGA/DTA) experiments were performed on a Polymer Laboratories STA 1500 instrument. Elemental analyses were performed under an argon atmosphere on a Perkin Elmer 2400 series II CHNS/O analyzer. The following compounds were used as received: strontium metal (Aldrich, Sr^0), strontium acetate (Fisher, $Sr(OAc)_2$), neo-pentyl alcohol (Aldrich, HONep), and *t*-butyl acetic acid (Aldrich, HONc).

$[Sr_2(\mu\text{-}ONc)_2(HONc)_4]_2$ (1)

In a vial, HONc (~5 mL) was added to $Sr(OAc)_2$ (0.251 g, 1.22 mmol). The reaction mixture was heated with stirring until a clear, pale yellow solution was obtained. The reaction was allowed to cool to room temperature, stirred for an additional 12 h, concentrated by rotary evaporation, and allowed to sit at glovebox temperatures until crystals formed (< 5 days). The resulting X-ray quality crystals proved to be $[Sr_2(\mu\text{-}ONc)_2(HONc)_4]_2$ (**1**). First crystalline yield 42.2% (0.402 g – final yields were not optimized). ^1H NMR (400.1 MHz, toluene-d_8) δ 12.56 (1.0H, bs, $\mathit{H}O_2CCH_2C(CH_3)_3$), 2.23 (4.1H, s, $O_2CC\mathit{H}_2C(CH_3)_3$, $HO_2CC\mathit{H}_2C(CH_3)_3$), 1.13 (19.9H, s, $O_2CCH_2\text{-}C(C\mathit{H}_3)_3$, $HO_2CCH_2C(C\mathit{H}_3)_3$). ^{13}C NMR (100 MHz, tol-d_8) δ 100.6 ($O_2\mathit{C}CH_2C(CH_3)_3$, $HO_2\mathit{C}CH_2C(CH_3)_3$), 50.1 ($O_2C\mathit{C}H_2C(CH_3)_3$, $HO_2\text{-}C\mathit{C}H_2C(CH_3)_3$), 31.0 ($O_2CCH_2\mathit{C}(CH_3)_3$, $HO_2CCH_2\mathit{C}(CH_3)_3$), 30.4 ($O_2CCH_2C(\mathit{C}H_3)_3$, $HO_2CCH_2C(\mathit{C}H_3)_3$). FT-IR (KBr pellet, cm^{-1} 2955(s), 2903(m), 2864(m), 2564(w), 1943(w), 1702(s), 1578(s), 1471(m), 1402(m), 1364(m), 1268(m), 1224(m), 1187(w), 1144(m), 1046(m), 961(w), 935(w), 900(w), 806(m), 788(w), 773(w), 739(m), 704(m), 647(m), 633(m), 611(w), 506(w), 478(m), 431(w). TGA/DTA (oxygen) (weight loss up to °C (% total weight loss)/thermal event, °C]: 125°C, 22.5%/sm endo (120°C), 200°C, 54.7%/sm endo (187°C), 448°C, 77.5%/lg exo (390°C). Elem. Anal. Calcd. for: (i) $C_{36}H_{68}O_{12}Sr$: Theoretical C, 55.40%; H, 8.78%; (ii) $C_{30}H_{56}O_{10}Sr$ (– 1 HONc): Theoretical C, 54.22%; H, 8.27%. Found C, 54.19%; H, 8.70%.

$Sr_5(\mu_4\text{-}O)(\mu_3\text{-}ONep)_4(\mu\text{-}ONep)_4(HONep)(solv)_4$ (solv = THF or MeIm)

Method A

In a Schlenk flask HONep (5.0 g, 16.5 mmol) was added to Sr^0 (1.0 g, 11.4 mmol) in THF (~ 15 mL) for **2a** (or MeIm for **2b**) and heated at reflux temperature for 48 h. After this time, all of the volatile materials were removed by vacuum distillation. Extraction with hot THF for **2a** (or toluene for **2b**) resulted in a clear yellow-tinged solution, which upon cooling, yielded X-ray quality crystals. For the THF solvent system the crystals proved to be $Sr_5(\mu_4\text{-}O)(\mu_3\text{-}ONep)_4(\mu\text{-}ONep)_4(HONep)(THF)_4$, **2a**. For the MeIm system the crystals proved to be $Sr_5(\mu_4\text{-}O)(\mu_3\text{-}ONep)_4(\mu\text{-}ONep)_4(HONep)\text{-}(MeIm)_4 \cdot (MeIm)_2(C_7H_8)$, **2b**.

Method B

A three-neck round-bottomed flask was charged with Sr^0 (21.7 g, 0.247 mol) fitted with two septa and a nitrogen adapter and then transferred to a Schlenk line that was attached to an NH_3(gas) cylinder. The flask was placed in an acetone/dry ice bath (–78°C) and fitted with a cold finger that was also cooled to –78°C. NH_3 gas was condensed (~ 250 mL) into the flask and the resulting blue solution was stirred for 1/2 h. HONep (75.6 g, 0.739 mol) dissolved in a separate Schlenk flask in THF/tol (50 : 50 mixture, ~125 mL) was syringed onto the dissolved Sr^0. The resulting mixture was manually stirred for 1/2 h and then allowed to warm to room temperature. The resulting off-white slurry had the volatile components removed *in vacuo* to yield a pale yellow powder that was redissolved in hot THF, dried by rotary evaporation to yield a pale yellow powder which was used without further purification. The analytical data of this material was consistent with the crystals of **2** isolated previously. Yield 88.9% (75.6 g). ^1H NMR (400 MHz, THF-d_8) δ 3.38 (2.57H, m, $\overline{OCH_2CH_2CH_2CH_2}$), 3.29 (1H, s, ONep), 2.99 (1.79H, s, ONep), 1.55 (3.08H, m, $\overline{OCH_2CH_2CH_2CH_2}$), 1.08 (7.89H, s, ONep), 0.66 (21.16H, s, ONep). $^{13}C\{^1H\}$(100.6 MHz, THF-d_8) δ 66.2 (O*Nep*), 27.6 (ONep), 26.1 (ONep). FT-IR (KBr pellet, cm^{-1}) 3622(w), 3516(w), 2959(mb), 2899(w), 2860(w), 1633(wb), 1481(mb), 1395(w, sh), 1322(w), 1262(w), 1222(w), 1156(w), 1096(m), 1017(m), 937(w), 891(w), 824(w), 705(w), 612(w), 559(w), 473(wb). Elem. Anal. Calcd. for $C_{61}H_{132}O_{14}Sr_5$: C, 47.96%; H, 8.70%. Found: C, 47.63%; H, 7.87%.

X-Ray Collection, Structure Determination, and Refinement

Compound 1

Colorless, square rods of **1** were immersed in a pool of mineral oil bathed in argon. A single crystal was then attached to a thin glass fiber using silicone grease and immediately placed under a liquid N_2 stream on a Siemens P4/PC diffractometer. Graphite monochromatized MoKα radiation (λ = 0.71073 Å) was used. The lattice parameters were optimized from a least-squares calculation on 25 carefully centered reflections of high Bragg angle. The data were collected using ω scans with a 1.80° scan range. Three check reflections monitored every 97 reflections showed no systematic variation of intensities. Lattice determination and data collection were carried out using XSCANS Version 2.10b software. All data reduction, including Lorentz and polarization corrections and structure solution and graphics were performed using SHELXTL PC Version 5.03 software. The structure refinement was performed using SHELX 93 software.† The data were corrected

---

†XSCANS and SHELXTL PC are products of Siemens Analytical X-ray Instruments, Inc., 6300 Enterprise Lane, Madison, Wisconsin 53719; (a) SHELX-93 is a program for crystal structure refinement written by G.M. Sheldrick (1993) University of Göttingen. Germany; (b) SHELXTL PC Version 4.2/360, 1994, Bruker Analytical X-ray Instruments, Inc., Madison, Wisconsin 53719; (c) SHELXTL Version 5.1, 1997, Bruker Analytical X-Ray Systems, 6300 Enterprise Lane, Madison, WI 53719.

TABLE I Data parameters for X-ray collection of: $[Sr(\mu\text{-}O_2CNep)_2(HO_2CNep)_4]_2$ (**1**), and $Sr_5(\mu_4\text{-}O)(\mu_3\text{-}ONep)_4(\mu\text{-}ONep)_5(HONep)(THF)_4$ (**2a**) and $Sr_5(\mu_4\text{-}O)(\mu_3\text{-}ONep)_4(\mu\text{-}ONep)_5(HONep)(py)_4 \cdot (MeIm)_2(toluene)$ (**2b**)

Compound	**1**	**2a**	**2b**
Chemical formula	$C_{72}H_{136}O_{24}Sr_2$	$C_{61}H_{132}O_{14}Sr_5$	$C_{61}H_{124}N_8O_{10}Sr_5 \cdot (C_4H_6N_2)_2(C_7H_8)$
Formula weight	1561.05	1483.41(1527.81)	1824.13
Temp. (K)	203	203	158
	Orthorhombic	Orthorhombic	Monoclinic
Space group	$Cmc2_1$	$Cmc2_1$	C2/m
a (Å)	21.304(5)	17.408(3)	23.0393(13)
b (Å)	21.448(4)	22.631(5)	18.4713(10)
c (Å)	23.061(3)	22.826(5)	22.8761(13)
α (°)			
β (°)			98.6140(10)
γ (°)			
V (Å^3)	10537.2(34)	8993(3)	9625.59(9)
Z	4	4	4
λ (MoKα radiation) (Å)	0.71073	0.71073	0.71073
D_{calcd} (mg/m^3)	0.987	1.128	1.259
μ (MoKα) (mm^{-1})	1.066	2.990	2.806
$R1$[a] (%)	8.98[c]	939[d]	15.10[e]
$wR2$[b] (%)	24.68	25.72	35.28
$R1$[a] (all data, %)	13.15[c]	11.94[d]	21.43[e]
$wR2$[b] (all data, %)	31.81	27.32	39.28

[a] $R1 = \sum||F_o| - |F_c||/\sum|F_o| \times 100$.

[b] $wR2 = [\sum w(F_o^2 - F_c^2)^2|\sum(w|F_o|^2)^2]^{1/2} \times 100$.

Final weighting scheme calculated:

[c] $w = 1/[\sigma^2(F_o^2) + (0.2118P)^2]$, [d] $w = 1/[\sigma^2(F_o^2) + (0.2000P)^2]$,

[e] $w = 1/[\sigma^2(F_o^2) + (0.1572P)^2 + 226.4793P]$ where $P = (F_o^2 + 2F_c^2)/3$.

for absorption using the ellipsoid option in the XEMP facility of SHELXTL PC. Data collection parameters are given in Table I.

The structure of **1** was solved in space group $Cmc2_1$ using direct methods and difference Fourier techniques. The strontium atom and the majority of all non-hydrogen atom positions were revealed. All hydrogen atoms were fixed in ideal geometries, with C–H distances of 0.97 (methylene), 0.96 (methyl), or 0.93 Å (aromatic). All hydrogen atoms were refined using the riding model in the HFIX facility in SHELXL 93. All hydrogen atoms had their isotropic temperature factors fixed at 1.2 (aromatic and methylene) or 1.5 (methyl) times the equivalent isotropic U of the atom they were bonded to. Ten peaks with F_o^2 much greater than F_c^2 were omitted; peak scans showed these peaks to be twinned. The carbon atom C(37) was refined with a weak ISOR restraint to keep it from going non-positive definite. The high residuals and anomalous bond distances in the structure are attributed to a small twin crystal. Solutions were also obtained in space groups Ama2 and

Cmcm, but refinements in these space groups proved to be more problematic. The final refinement included anisotropic thermal parameters on all non-hydrogen atoms and converged to $R1 = 0.0898$ and $R2_w = 0.2468$.

Compound 2a

An irregularly shaped, colorless crystal of **2a** was mounted using standard air sensitive handling techniques (*vide infra*). The data were collected on a Bruker P_4/CCD/PC diffractometer, with a sealed MoKα X-ray source. A hemisphere of data was collected using a combination of ϕ and ω scans, with 30 s exposures and 0.3 frame widths. The final cell was determined from a least-squares refinement on 8192 reflections. Data collection, indexing, and initial cell refinement were handled using SMART software.[‡] Frame integration and final cell refinement were carried out using SAINT software.[§] The SADABS software package was used to perform the absorption corrections.[||]

The structure was solved in the space group Cmc2_1 using direct methods and difference Fourier techniques. This solution yielded all of the strontium and oxygen atom positions. A refinement, with all strontium and oxygen atoms refined anisotropically, converged to $R1$ (14%). Subsequent location of ONep and THF ligand carbon atoms was problematic due to disorder in the crystal structure. Fragment models for the THF and ONep ligands were constructed using literature coordinates. The FRAG command within SHELXTL was used to constrain the ligands to ideal geometry which resulted in a final $R1 = 9.4\%$. The final refinement included anisotropic temperature factors on Sr and O atoms only, and H atom positions were not considered. The temperature factors on Sr and O atoms were well behaved, but the C atom temperature factors were, on average, abnormally large. These large temperature factors are attributed to extreme disorder and/or *pseudo*-symmetry. Additional refinements were attempted in the space groups Cmcm and Ama2, but this did not improve the model. The structure was refined as a racemic twin, and the absolute structure (Flack) parameter refined to 0.562(4). Structure solution, refinement, graphics, and creation of publication materials were performed using SHEXTL 5.1 software.[¶] Additional details of data collection, and structure refinement are given in Table I.

[‡] SMART Version 4.210, 1997, Bruker Analytical X-Ray Systems Inc., 6300 Enterprise Lane, Madison, WI 53719.

[§] SAINT Software Users Guide, Version 4.05, 1997, Bruker Analytical X-Ray Systems, 6300 Enterprise Lane, Madison, WI 53719.

[||] SADABS George M. Sheldrick, 1997 Brucker Analytical X-Ray Systems, Inc.: Madison WI.

[¶] See foot note[†].

RESULTS AND DISCUSSION

Initial attempts to generate Sr precursors with increased solubility were realized through the introduction of larger sterically hindering ligands that possessed the Nep hydrocarbon chain, HONc and HONep (Figure 1). The synthesis, solid state, and solution behavior of these derivatives are described in detail.

Synthesis

The carboxylate ligands of $Sr(OAc)_2$ were readily metathesized by dissolution of the starting material in excess of the desired HORc (equation (1)). A number of sterically varied commercially available HORc were investigated. The HONc substituent was of particular interest due to the presence of the Nep hydrocarbon moiety. The metathesis of the OAc for the ONc ligand was accomplished by heating a mixture of $Sr(OAc)_2$ in excess HONc until the solution became clear

$$Sr(OAc)_2 + (XS)\ HONc \rightarrow Sr(ONc)_2 + 2HOAc \qquad (1)$$

whereupon the heat was removed and the reaction was stirred overnight. After 12 h, the mixture was allowed to sit at glovebox temperatures until crystals formed (~ 1–2 days) which proved to be $[Sr(\mu\text{-}ONc)_2(HONc)_4]_2$ (**1**). The ball and stick plot of **1** is shown in Figure 2. The elemental analysis of this material from sample to sample was inconsistent; however, the majority of the analyses had a stoichiometry consistent with "$Sr(ONc)_2\text{-}(HONc)_3$". The volatility of the weakly coordinated HONc solvent upon heating would account for the variable analytical data.

For the production of the alkoxide derivatives, Sr^0 metal was reacted with the parent alcohol (HONep) in THF at reflux temperatures:

$$Sr + HONep \xrightarrow{THF} \mathbf{2a} \qquad (2)$$

The reaction from equation (2) was heated until a majority of the metal had been consumed. The volatile component of this reaction mixture was removed by vacuum distillation to yield a white powder. Upon extraction with hot THF, followed by slow cooling to room temperature, X-ray quality crystals were isolated which proved to be $Sr_5(O)(ONep)_8(HONep)(THF)_4$, **2a**. Figure 3(a) shows the central core of **2a**. Low yields of **2a** were drastically improved by exposing fresh surfaces of the Sr^0 under inert

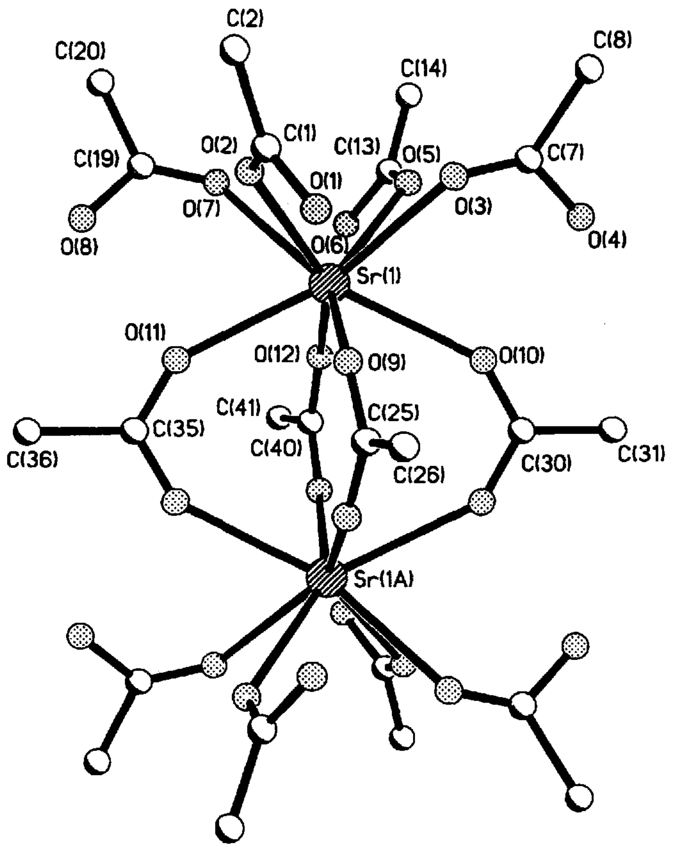

FIGURE 2 Ball and stick plot of 1. The *t*-butyl groups have been removed for clarity.

atmospheric conditions prior to introduction into the reaction. With careful and rapid handling of the crystals, we were able to obtain several elemental analyses with acceptable percentages; however, due to the volatility of the solvent ligands, a wide range of results was also noted. In an attempt to further reduce the oligomerization of **2a**, an alternative strong Lewis basic solvent, MeIm, was used in place of THF. A similar synthesis and crystallization was performed as noted for **2a** (see equation (2)). X-ray crystallography indicated that an identical structural arrangement was adopted with the MeIm replacing the THF bound solvent molecules (additional solvent molecules of MeIm and toluene were located in the unit cell). Figure 3(b) shows the thermal ellipsoid plot of the central core of **2b**.

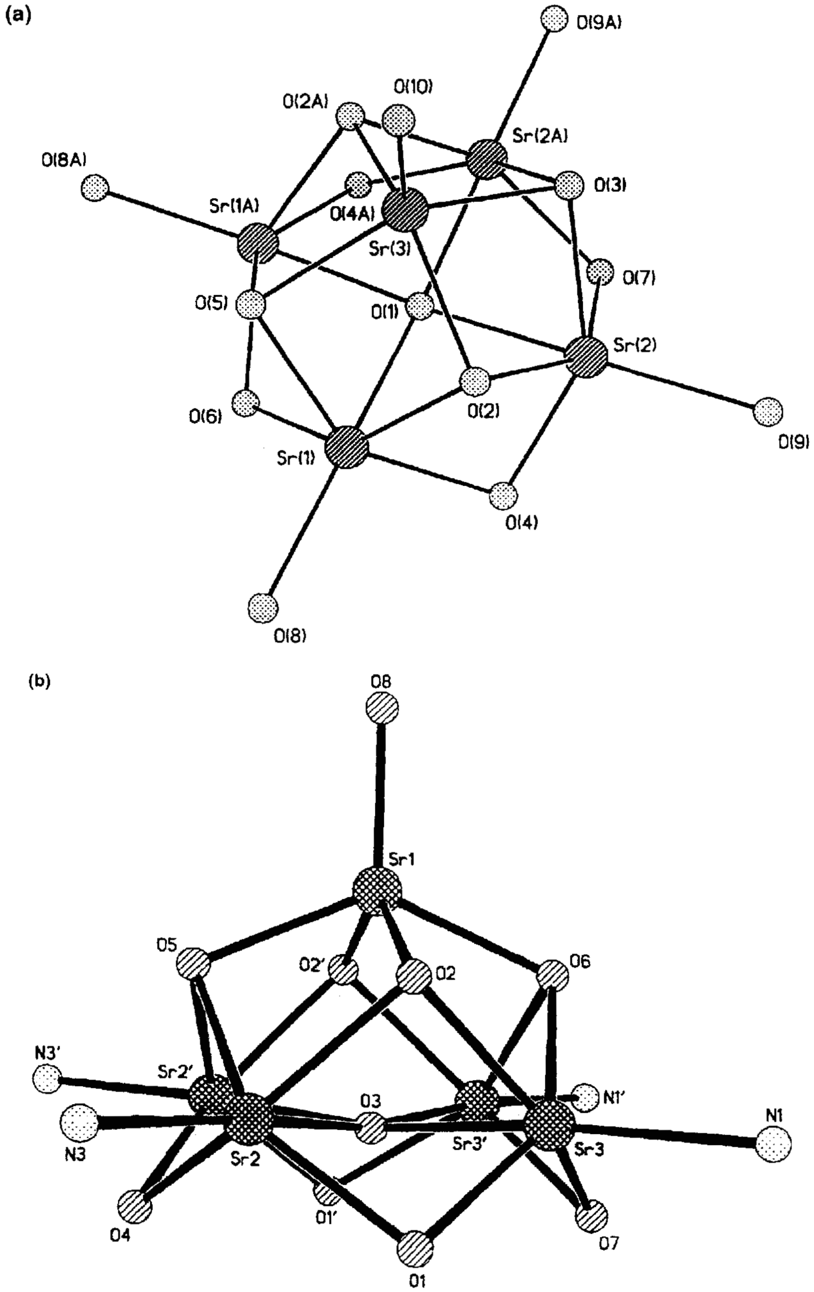

FIGURE 3 Ball and stick plot of the central core of (a) **2a** and (b) **2b**.

Solid State

Crystal Structure

While there are a number of reports detailing the preparation of Sr containing alkoxide or acetate compounds, few report the structure of these precursors. In order to fully exploit these compounds it is necessary to know their structure; hence we initiated solid state characterization of **1**, **2a**, and **2b** (Table II).

The few strontium carboxylate complexes that have been crystallographically characterized include the following: $[Sr_2(\mu\text{-}OAc)_2(OAc)_2(H_2O)]_\infty$,[29] $\{[Sr(OAc)_2(H_2O)_2][H_2(OAc)_3]\}_\infty$,[30] and $\{[Sr(OAc)(H_2O)_2][H(OAc)_2]\}_\infty$.[31] These species exhibit a wide range of coordination six to nine numbers for Sr metal centers. The mixed ligated species $[Sr_2(OAc)_2(NO_3)_2(H_2O)_3]$[32] has also been structurally characterized. For each of the bound acetate ligands in the above compounds, the acetate moieties act as either a chelating or chelating-bridging ligand.

Figure 2 shows the solid state structure of **1** wherein each of the eight-coordinated metal cations adopt a unique distorted square anti-prism geometry for Sr. The Sr metal centers of this molecular complex are joined through four monodentate μ-ONc ligands with the remaining coordination sites being filled by monodentate (terminal) HONc solvent molecules. Since all of the ORc ligands act as unidentate bridging moieties, the bite angle of the acetate ligands $[(\mu\text{-}O)\text{–}C\text{–}(\mu\text{-}O)]$ would be expected to be significantly elongated in comparison to those angles observed for other ORc species of Sr; however, the $(\mu\text{-}O)\text{–}C\text{–}(\mu\text{-}O)$ angles of **1** are consistent with the previously reported bite angle (119.9°–124°) range. This may be accounted for by the large size (Sr^{2+}: 1.32–1.58 Å)[33] of the Sr cation which does not require constraint of the ONc ligand; thus, the energetically relaxed state of the ONc ligand exists whether chelating or bridging. It was observed that the constrained ONc ligands have a small range for their bite angle (121°–123°) and that the terminal ONc vary through a larger range (119°–125°). The Sr–O distances of **1** (av. 2.60 Å) are in agreement with literature reports. The Sr(1)–O(5) distance of 2.74 Å is one of the longest Sr–O bonds reported for carboxylate derivatives.

The structures of several $Sr(OR)_2$ complexes have been reported in the literature: $[Sr(OMe)_2]_\infty$ (no molecular subunits),[34–36] $[Sr(OEt)_2(HOEt)_4]_\infty$,[36] and $Sr_4(OPh)_8(PhOH)_2(THF)_6$.[37] The first two were poorly characterized by powder diffraction studies and the latter successfully introduced large sterically hindering aryloxides to avoid polymeric structures.

TABLE II Select bond distances (Å) and angles (°) for **1**, **2a**, and **2b**

	1		**2a**		**2b**	
Distance (Å)						
Sr–Sr	Sr(1)–Sr(1a)	4.498(2)	Sr(1)–Sr(1a)	3.573(3)	Sr(1)–Sr(2)	3.729(2)
			Sr(2)–Sr(2a)	3.581(3)	Sr(1)–Sr(3)	3.723(2)
					Sr(2)–Sr(2a)	3.586(2)
					Sr(2)–Sr(3)	3.577(2)
					Sr(3)–Sr(3a)	3.585(2)
Sr–(μ_4-O)						
Apical	—		Sr(3)–O(1)	2.974(12)	Sr(1)–O(3)	2.952(9)
Basal			Sr(1)–O(1)	2.543(11)	Sr(2)–O(3)	2.538(6)
			Sr(2)–O(1)	2.539(11)	Sr(3)–O(3)	2.546(6)
Sr–(μ_3-ONep)						
Apical	—		Sr(3)–O(3)	2.549(17)	Sr(1)–O(2)	2.496(9)
			Sr(3)–O(2)	2.497(12)	Sr(1)–O(5)	2.476(10)
			Sr(3)–O(5)	2.506(15)	Sr(1)–O(6)	2.489(10)
Basal			Sr(1)–O(2)	2.516(11)	Sr(2)–O(2)	2.532(7)
			Sr(1)–O(5)	2.538(10)	Sr(2)–O(5)	2.553(7)
			Sr(2)–O(2)	2.555(13)	Sr(3)–O(2)	2.537(8)
			Sr(2)–O(3)	2.69(3)	Sr(3)–O(6)	2.543(7)
Sr–(μ-ONep)	—		Sr(1)–O(4)	2.50(1)	Sr(2)–O(1)	2.438(9)
			Sr(1)–O(6)	2.58(2)	Sr(2)–O(4)	2.447(6)
			Sr(2)–O(4)	2.39(1)	Sr(3)–O(1)	2.463(8)
			Sr(2)–O(7)	2.65(2)	Sr(3)–O(7)	2.450(7)
Sr–(μ-ONc)	Sr(1)–O(9)	2.531(11)	—		—	
	Sr(1)–O(10)	2.625(12)				
	Sr(1)–O(11)	2.513(12)				
	Sr(1)–O(12)	2.599(10)				
Sr–O(solv)	Sr(1)–O(2)	2.543(13)	—		—	
	Sr(1)–O(3)	2.675(15)				
	Sr(1)–O(5)	2.741(13)				
	Sr(1)–O(7)	2.586(11)				

Angles (°)						
O_{term}–Sr–O_{term}	O(2)–Sr(1)–O(3)	69.2(4)	—			
	O(2)–Sr(1)–O(5)	106.2(4)				
	O(2)–Sr(1)–O(7)	70.2(4)				
	O(3)–Sr(1)–O(5)	67.6(4)				
	O(3)–Sr(1)–O(7)	106.9(3)				
	O(5)–Sr(1)–O(7)	69.2(4)				
(μ-O)–Sr–(μ-O)	O(9)–Sr(1)–O(10)	76.3(4)	O(6)–Sr(1)–O(4)	111.3(5)	O(1)–Sr(2)–O(4)	111.5(4)
	O(9)–Sr(1)–O(11)	80.4(4)	O(4)–Sr(2)–O(7)	110.6(5)	O(1)–Sr(3)–O(7)	110.7(4)
	O(9)–Sr(1)–O(12)	126.5(3)			O(7)–Sr(3a)–O(1a)	
	O(10)–Sr(1)–O(11)	126.2(3)			O(4)–Sr(2a)–O(1a)	
	O(10)–Sr(1)–O(12)	76.0(4)				
	O(11)–Sr(1)–O(12)	80.5(4)				
(μ_3-O)–Sr–(μ-O)	—		O(2)–Sr(1)–O(4)	75.3(4)	O(2)–Sr(2)–O(1)	72.0(4)
			O(2)–Sr(1)–O(6)	140.1(6)	O(2)–Sr(2)–O(4)	143.8(3)
			O(5)–Sr(1)–O(4)	143.6(4)	O(5)–Sr(2)–O(1)	143.6(3)
			O(5)–Sr(1)–O(6)	73.3(6)	O(5)–Sr(2)–O(4)	75.4(3)
			O(2)–Sr(2)–O(4)	76.4(4)	O(2)–Sr(3)–O(1)	74.5(2)
			O(2)–Sr(2)–O(7)	140.2(5)	O(2)–Sr(3)–O(7)	143.8(3)
			O(3)–Sr(2)–O(4)	143.7(5)	O(6)–Sr(3)–O(1)	143.5(3)
			O(3)–Sr(2)–O(7)	71.43(5)	O(6)–Sr(3)–O(7)	75.6(3)
(μ_3-O)–Sr–(μ_3-O)			O(2)–Sr(1)–O(5)	79.6(4)	O(2)–Sr(3)–O(6)	79.1(3)
			O(2)–Sr(2)–O(3)	80.4(5)	O(2)–Sr(2)–O(5)	78.6(3)
			O(2)–Sr(3)–O(5)	80.6(3)	O(5)–Sr(1)–O(2)	80.7(2)
			O(3)–Sr(3)–O(5)	132.1(5)	O(2)–Sr(1)–O(6)	80.7(2)
(μ-O)–C–(μ-O)	O(9)–C(25)–O(9a)	121.0(22)	—		—	
	O(10)–C(30)–O(10a)	120.2(28)				
	O(11)–C(35)–O(11a)	120.8(19)				
	O(12)–C(40)–O(12a)	123.6(20)				
O_{term}–C–O	O(1)–C(1)–O(2)	125.0(19)	—		—	
	O(3)–C(7)–O(4)	124.1(20)				
	O(5)–C(13)–O(6)	119.5(19)				
	O(7)–C(19)–O(8)	123.5(17)				
Sr–(μ_4-O)–Sr			Sr(1)–O(1)–Sr(2)	89.67(7)	Sr(2)–O(3)–Sr(2a)	89.9(3)
			Sr(1)–O(1)–Sr(1a)	89.3(5)	Sr(2)–O(3)–Sr(3a)	170.1(4)
			Sr(1)–O(1)–Sr(2a)	170.1(5)	Sr(2)–O(3)–S(3)	90.0(2)
			Sr(2)–O(1)–Sr(1a)	170.1(5)	Sr(2a)–O(3)–Sr(3a)	89.4(1)
			Sr(2)–O(1)–Sr(2a)	89.7(5)	Sr(2a)–O(3)–Sr(3)	170.1(4)
			Sr(2a)–O(1)–Sr(1a)	89.67(7)	Sr(3a)–O(3)–Sr(3)	89.5(3)

We have successfully isolated the first "$Sr(OR)_2$" that has been characterized by single crystal X-ray analysis using the simple sterically demanding ONep ligand.

The central cores of **2a** and **2b** are shown in Figure 3(a) and (b), respectively. Both compounds consist of four Sr cations arranged in a square geometry surrounding a μ_4-O ligand. An additional Sr cation is located directly above the μ_4-O but the distance is too great to be considered a bond. The Sr atoms are thus arranged in a square-based pyramidal (sp) geometry around a μ_4-O. There are four μ_3-ONep ligands on each face of the pyramid linking three Sr atoms. On the base of the skeletal arrangement of Sr atoms; four μ-ONep ligands bridge between the metals. To complete the octahedral (O_h) geometry of the Sr atoms, solvent molecules are terminally coordinated. For **2a**, the solvent molecules are a mixture of HONep and THF ligands, whereas, for **2b** MeIm replaces the THF ligands. Furthermore, significant disorder in the apically bound HONep solvent molecule for both **2a** and **2b** which is most likely a representation of the HONep being present in more than one position on the molecule and the forced mirror plane that occurs for these space groups. For these compounds, the HONep ligand was always isolated in the apical position, regardless of the solvent introduced. Furthermore, for **2b**, the unit cell solvent molecules are very disordered and reduce the reliability of the metrical data noted for the external ligands of this structure. The structures of **2** and **3** are reminiscent of the $Y_5(O)(OPr^i)_{13}(HOPr^i)_5$ complex previously isolated by Hubert-Pfalzgraf and co-workers.[38]

Due to the solvent molecule disorder little discussion concerning the distances and angles associated with the peripheral ligands will be presented; however, the core arrangement of **2a** and **2b** are very well defined and the metrical data are sufficiently reliable to warrant discussion. The basal Sr–O distances of **2a** and **2b** av. 2.54 Å. The apical Sr–O distance of **2a** (2.982(14) Å) and **2b** (2.95 Å) are longer than what is acceptable for a Sr–O bond. However, some interaction is expected due to the propensity of Sr to adopt high coordination numbers. The square base pyramidal central core is irregular which is in contrast to the very regular arrangement of the $Y_5(O)(OPr^i)_{13}(HOPr^i)_5$ complex. The Y_5–(μ_4-O) distances are statistically equivalent.[38] The basal $Sr_4(\mu_4\text{-}O)$ plane should ideally possess four 90° angles and two 180° angles. The 90° angles are present for **2a** and **2b**; however, the 180° angles are reduced to 170° angles which removes the O(1) atom from the plane of the Sr atoms. Each $[Sr–O]_2$ square was found to be elongated, further distorting the sp central core. Furthermore, for the Y_5–(μ_5-O) structure it was reported that the Y–(μ_3-O) distances were shorter for the apical than the basal metals. In contrast, **2a** and **2b** have statistically similar distances reported for all of the Sr–(μ_3-ONep) distances but the Sr–(μ-ONep) distances vary significantly. As is often observed in metal alkoxides, increased binding of the alkoxide leads to longer bonds: for **2a**, Sr–(μ-OR), av. 2.45 Å > Sr–(μ_3-OR), av. 2.53 Å and for **2b**, Sr–(μ-OR), av. 2.46 Å > Sr–(μ_3-OR), av. 2.52 Å.

FT-IR Spectroscopy

The FT-IR spectrum of **1** has two types of carboxylate ligands present at 1693 and 1573 cm^{-1} that differ from the starting HONc carboxylate stretch at 1706 cm^{-1}. The multiplicity and consistency between **1** and HONc indicates that the 1693 cm^{-1} stretch most likely represents the terminally bound HONc ligands and the more encumbered μ-ONc ligand stretches are shifted to a higher frequency at 1573 cm^{-1}. The Sr–O stretches were noticeably weak in the spectrum of **1** in comparison to **2a** and **2b**.

The FT-IR spectra of **2a** and **2b** are, as expected, nearly identical. The ONep ligand stretches dominate the spectra with minor differences associated with the different solvents THF and MeIm that are coordinated. There is a relatively strong peak present around 550 cm^{-1} for both samples which may be indicative of the Sr–(μ_4-O) stretches associated with these compounds.

Solution State

Molecular Weight Determinations

Solution molecular weight (MW) determinations by the Signer method[39] were undertaken to determine the nuclearity of **1** which was found to be on av. 754 ± 26. This is approximately 1/2 of the solid state structure (MW = 1561.1). The solution MW of **2a** and **2b** were not undertaken due to their low solubility in toluene.

NMR Spectroscopy

Crystals of **1**, **2a**, and **2b** were dried by rotary evaporation at room temperature and then redissolved in toluene-d_8 to elucidate their solution behavior. All samples were prepared as concentrated as possible to minimize dynamic solution behavior.

The ^{1}H NMR spectrum of **1** consists of only one set of ONc resonances (δ 12.56, 2.23, and 1.13 ppm) which are significantly shifted from the starting acid (HONc: δ 12.29, 1.98, 0.93). This spectrum can be interpreted as either the solid state structure of compound **1** is: (i) retained with rapid exchange of the terminal and bridging ONc ligands or (ii) disrupted to form a mononuclear species. If the former were true, low temperatures should slow the exchange; however, variable temperature NMR spectra did not show new peaks except at −90°C, whereupon, a shoulder on the methyl peak was observed. Over the same temperature range the methylene peak broadens and shifts slightly but no peak deconvolution was observed. For the acidic proton, the peak shifts from δ 12.5 at room temperature to 15.1 ppm at −90°C but remains a broad singlet. Due to the lack of observable bridging and terminal ligand exchange, the NMR data (and the MW determination) indicate that **1** adopts a mononuclear complex in solution.

The NMR spectrum recorded for **2a** in THF-d_8 is very simple with only two resonances observed (δ 3.27 and 0.81). The ONep resonances consist of one sharp and one broad set of resonances in an approximate 1 : 3 ratio. This is not consistent with the solid state structure and some dynamic behavior must be associated with **2a**. Exchange of half of the μ_3-ONep ligands with the μ-ONep ligands would yield a spectrum consistent with the observed ratio and could be easily envisioned (see Figure 4). VT-NMR spectroscopy (25°C to −100°C) revealed a number of resonance changes in the methylene region but no new peaks were observed. The methyl region displayed a number of new resonances that appear at 0°C and continue to sharpen and change chemical shifts as lower temperatures are approached.

The ^{1}H NMR spectrum of **2b** was collected in C_6D_6 and proved very similar to that of **2a** with the inclusion of MeIm peaks at δ 7.45, 7.37, 6.28, 2.61 ppm. In the methylene reion at least seven peaks are identifiable with

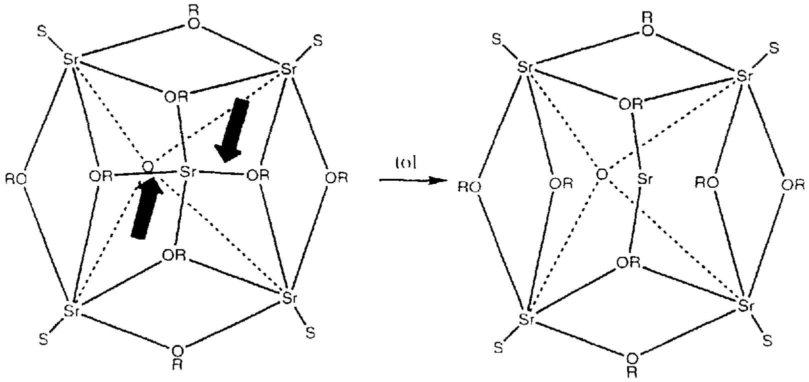

FIGURE 4 Schematic representation of the solid state and proposed solution state structure of **2a**.

up to five methyl resonances. If the structure is asymmetric in solution then eight types of ONep resonances should be present. Furthermore, with the more Lewis basic MeIm solvent donating more electron density to the metal, it is less likely that disruption of the μ_3-ONep ligands observed in the solid state would occur in solution. Therefore, these data indicate that the MeIm structure remains intact in solution.

CONCLUSION

We have successfully isolated and characterized two novel Sr complexes that demonstrate increased solubility in organic solvents when compared to commercially available precursors. These include a solvated dinuclear complex as observed for **1** and a penta-nuelear arrangement of Sr atoms around a μ_4-O atom recorded for **2a** and **2b**. The increased solubility of **1**, **2a**, and **2b** is a result of decreased oligomerization induced by the steric bulk of the Nep pendant hydrocarbon chains along with the coordination of solvent molecules. NMR and MW determinations indicate that **1** is mononuclear in solution, while, NMR data indicate that **2a** and **2b** maintain their general nuclearity in solution with rapid ligand exchange.

Acknowledgments

Sandia is a multi-program laboratory operated by Sandia Corporation, a Lockheed Martin Company, for the United States Department of Energy. The authors would like to thank K.A. Krause for her technical assistance.

Supporting Information

A complete list of data acquisition and thermal parameter listing is supplied (53 pages). Information concerning obtaining this material is listed on any current masthead.

References

[1] T.J. Boyle, H.N. Al-Shareef, C.D. Buchheit, R.T. Cygan, D. Dimos, M.A. Rodriguez, B. Scott and J.W. Ziller, *Integrated Ferroelectrics*, **18**, 213 (1997).

[2] T.J. Boyle, P.G. Clem, M.A. Rodriguez, B.A. Tuttle and M.D. Heagy, *J. Sol–Gel Sci. Tech.*, **16**, 47 (1999).

[3] T.J. Boyle, C.D. Buchheit, M.A. Rodriguez, H.N. Al-Shareef, B.A. Hernandez, B. Scott and J.W. Ziller, *J. Mater. Res.*, **11**, 2274 (1996).

[4] M.A. Rodriguez, T.J. Boyle, B.A. Hernandez, C.D. Buchheit and M.O. Eatough, *J. Mater. Res.*, **11**, 2282 (1996).

[5] M.A. Rodriguez, T.J. Boyle, C.D. Buchheit, C.A. Drewien, B.A. Hernandez and M.O. Eatough, *Integrated Ferroelectric*, **14**, 201 (1997).
[6] K.A. Jose, V.K. Varadan and V.V. Varadan, *Microwave Opt. Tech. Lett.*, **20**, 166 (1999).
[7] S. Kumar, G.L. Messing and W.B. White, *J. Am. Ceram. Soc.*, **76**, 617 (1993).
[8] S. Saha and S.B. Krupanidhi, *Mater. Sci. Engin. B, Solid State Mater. Adv. Tech.*, **57**, 135 (1999).
[9] M.S. Tsai, S.C. Sun and T.Y. Tseng, *J. Am. Ceram. Soc.*, **82**, 351 (1999).
[10] S. Yamamichi, A. Yamamichi, D.G. Park, T.J. King and C.M. Hu, *IEEE Trans. Electron Dev.*, **46**, 342 (1999).
[11] P.C. Joshi, S.O. Ryu, X. Zhang and S.B. Desu, *J. Korean Phys. Soc.*, **32**, S1583 (1998).
[12] K. Kato, J.M. Finder, S.K. Dey and Y. Torii, *Integrated Ferroelectrics*, **18**, 237 (1997).
[13] I. Koiwa, K. Tani, J. Mita and T. Iwabuchi, *Jap. J. Appl. Phys. Part 1*, **37**, 192 (1998).
[14] C.D.E. Lakeman, T.J. Boyle and M.A. Rodriguez, *Integrated Electronics*, **22**, 565 (1998).
[15] J.-S. Lee, J.-W. Park, J.-S. Park, H.-D. Park and S.-M. Shin, *J. Mater. Sci. Lett.*, **16**, 941 (1997).
[16] K.B. Lee, H.S. Lee and S.K. Cho, *J. Korean Phys. Soc.*, **32**, S1565 (1998).
[17] T. Noguchi, T. Hase and Y. Miyasaka, *Jpn. J. Appl. Phys. Part 1*, **9B**, 4900 (1996).
[18] T.J. Boyle, D.M. Pedroity, B.L. Scott and J.W. Ziller, *Polyhedron* **17**, 1959 (1997).
[19] T. Osaka, S. Ono, A. Sakakibara and I. Koiwa, *IEICE Trans. Elect.*, **E81C**, 545 (1998).
[20] N.J. Seong, E.S. Choi and S.G. Yoon, *J. Vacuum Sci. Tech. A Vacuum Surf. Films*, **17**, 83 (1999).
[21] N.J. Seong and S.G. Yoon, *Phys. IV*, **8**, 255 (1998).
[22] M. Elbouanani, I.F. Bubb, J.F. Scott, D.D. Cohen, N. Dytlewski and J.W. Martin, *Integrated Ferroelectrics*, **16**, 159 (1997).
[23] T.C. Chen, C.L. Thio and S.B. Desu, *J. Mater. Res.*, **12**, 2628 (1997).
[24] T.C. Chen, T.K. Li, X.B. Zhang and S.B. Desu, *J. Mater. Res.*, **12**, 1569 (1997).
[25] T.J. Boyle, U.S. Patent 5 683 614, 1997.
[26] D.C. Bradley, R.C. Mehrotra and D.P. Gaur, *Metal Alkoxides*, Academic Press: New York, 1978.
[27] T.J. Boyle, T.A. Alam, D. Dimos, G.J. Moore, C.D. Buchheit, H.N. Al-Shareef, E.R. Mechenbier and B.R. Bear, *Chem. Mater.*, **9**, 3187 (1997).
[28] T.J. Boyle, D.M. Pedrotty, C.J. Tafoya and J.W. Ziller, *Abstracts of Papers of the Am. Chem. Soc.*, **215**(pt.1), 521-INOR (April 2, 1998).
[29] C.J. Groombridge, R.K. Harris, K.J. Packer, M.B. Hursthouse and N.P.C. Walker, *J. Solid St. Chem.*, **59**, 306 (1985).
[30] V.K. Trunov, N.O. Endeladze and V.A. Efremov, *Zh. Strukt. Khim.*, **29**, 104 (1988).
[31] V.K. Trunov, A.D. Chubinidze, V.A. Efremov and Y.A. Velikodnyi, *Koord. Khim.*, **10**, 403 (1984).
[32] C.L. Lengauer and G. Giester, *Acta Cryst. Sec. C. Crystal Structure*, **53**, 870 (1997).
[33] R.D. Shannon, *Acta Cryst.* **A32**, 751 (1976).
[34] H.D.Z. Lutz, *Anorg. Allg. Chem.* **353**, 207 (1967).
[35] H. Staeglich and E. Weiss, *Chem. Ber.*, **111**, 901 (1978).
[36] N. Ya, B.A. Turova, A. Popovkin and A.V. Novoselova, *Dokl. Aka. Nauk SSSR*, **167**, 604 (1966).
[37] R.S. Drake, W.E. Streib, M.H. Chisholm and K.G. Caulton, *Inorg. Chem.*, **29**, 2707 (1990).
[38] O. Poncelet, W.J. Sartain, L.G. Hubert-Pfalzgraf, K. Folting and K.G. Caulton, *Inorg. Chem.*, **28**, 263 (1989).
[39] E.P. Clark, *Analytical Ed.*, 820 (1941).